Development of an optically gated math xmlns="http://www.w3.org/1998/Math/MathML">mrow>mi >Fe/mi>mo>//mo>mi>n/mi>mtext>-GaAs/mtext> /mrow>/math> spin-polarized transistor

J. Y. Kim, M. Samiepour, E. Jackson, J. Ryu, D. Iizasa, T. Saito, M. Kohda, J. Nitta, H. E. Beere, D. A. Ritchie, and A. Hirohata

Phys. Rev. B **106**, 134404 — Published 7 October 2022

DOI: 10.1103/PhysRevB.106.134404

Development of an Optically-Gated Fe/*n*-GaAs Spin-Polarised Transistor

J. Y. Kim,[1),2)] M. Samiepour,[3),a)] E. Jackson,[3),b)] J. Ryu,[4),c)] D. Iizasa,[4)] T. Saito,[4)] M. Kohda,[4),5),6)] J. Nitta,[4),5),6)] H. E. Beere,[7)] D. A. Ritchie,[7)] and A. Hirohata [3),*]

[1] *Department of Physics, University of York, York, YO10 5DD, United Kingdom*

[2] *Institute of Materials Research and Engineering, Agency for Science, Technology and Research (A*STAR), 138634, Singapore*

[3] *Department of Electronic Engineering, University of York, York, YO10 5DD, United Kingdom*

[4] *Department of Materials Science, Tohoku University, Sendai 980-8579, Japan*

[5] *Spintronics Research Network, Tohoku University, Sendai 980-8579, Japan*

[6] *Organisation for Advanced Studies, Center for Science and Innovation in Spintronics (Core Research Cluster), Tohoku University, Sendai 980-8579, Japan*

[7] *Department of Physics, University of Cambridge, Cambridge, CB3 0HE, U.K.*

[a)] *Present address: Seagate Technology, Londonderry BT48 0LY, United Kingdom*

[b)] *Present address: Oxford Instruments, Abingdon OX13 5QX, U.K.*

[c)] *Present address: Samsung Advanced Institute of Technology, Suwon 16678, Republic of Korea*

[*] *E-mail: atsufumi.hirohata@york.ac.uk*

Abstract

Efficient modulation of electrically-injected spin signals that is suitable for modern-day transistor functionality is yet to be established. In this work, we demonstrate in detail the fabrication of Fe/*n*-GaAs spin injection device and the experimental setup for an optical gating of the non-local spin transport signal. *In-situ* SEM interface imaging reveals more uniform current distribution at the Fe/*n*-GaAs injector interface at bias voltages higher than the Schottky barrier height. Three- and four-terminal Hanle measurements confirm successful spin injection into *n*-GaAs, with strong interfacial spin dephasing at high magnetic fields. Time-resolved pump-probe Kerr rotation setup was used to illuminate circularly-polarised light in the region of the pure spin current in Fe/*n*-GaAs lateral spin injection devices, where (0.4 ± 0.3)% modulation of the non-local signal depending on the light helicity was observed at 30 K.

Introduction

Spin-polarised field-effect transistor (spin FET) [1] is a critical vehicle to study injection, manipulation and detection of spin-polarised electrons in a semiconductor. As originally proposed, a two-dimensional electron gas in a semiconductor has been widely exploited as a possible medium for a spin FET due to its high in-plane carrier mobility. In particular, the Fe/GaAs system has been intensely investigated thanks to the very small lattice mismatch, where successful injection and detection of electron spins have been reported [2,3]. Theoretically the Fe/GaAs(001) and Fe/ZnSe(001) interfaces were calculated to achieve a spin polarisation of 99% by the coherent tunnelling [4]. Experimentally Crooker *et al.* measured the spin polarisation of 32% at an Fe/GaAs Schottky junction [5], and also reported distributions in the reversal of spin polarisation with respect to the applied bias, which can be caused by spin transport through an interfacial resonant state as theoretically predicted [6]. To avoid such inconsistency in devices, Fleet *et al.* succeeded to grow an abrupt Fe/GaAs(001) interface epitaxially using cold deposition at ~ 173 K, confirming reproducible spin-polarised current injection without bias-dependent reversal [7]. Using InAs, which forms almost negligible depletion layer at the interfaces and edges, successful spin injection was also demonstrated at 75 K [8], followed by spin injection into Si [9].

However, modulation of the injected spins via electromagnetic gating is still required to create a working spin FET. Recently electrical field operation has been demonstrated in InAs quantum well, where 360º rotation in 1.2 μm was achieved at 1.8K [10], which was not suitable for the device-level miniaturisation. This is because of the limitation in a spin-orbit interaction constant, which is unique to a semiconducting material [11]. We have accordingly proposed optical gating to achieve more effective spin modulation in GaAs [12].

In this study, we successfully fabricated four-terminal Fe/*n*-GaAs spin injection devices and performed optical gating experiment at 30 K. Signs of systematic variation of non-local spin voltage depending on the optical gating polarization were observed, indicating non-local spin accumulation could be modified with spins of optically injected charge carriers. *In-situ* SEM interface imaging of the Fe/GaAs injector interface was also used to reveal bias-dependence of charge transport uniformity across the injector interface.

Experimental Procedures

Firstly, careful design of *n*-doped GaAs stacks were required to enable efficient electrical spin injection. The GaAs modulation-doped stacks were grown by molecular beam epitaxy (MBE) in the Semiconductor Physics Group in the University of Cambridge. On a semi-insulating GaAs(001) substrate, 250 nm of GaAs buffer layer was deposited, followed by 2 μm of lightly-doped ($n = 2 \times 10^{16}$ cm^{-3}, Si dopants) *n*-GaAs as the main conducting channel.

In order to create sharp Schottky barriers at the Fe/GaAs interface with a narrow (< 20 nm) depletion region, required for efficient electrical spin injection, further 15 nm of modulation (n = 2×10^{16} cm^{-3} → 5×10^{18} cm^{-3}) followed by 15 nm of highly-doped (n = 5×10^{18} cm^{-3}) layer were deposited on top of the channel layer. The sharp, ~10 nm wide Schottky barrier formation was confirmed using a 1-dimensional Poisson/Schrödinger solver [13], as shown in Supplemental Material Section I [14]. The stacks were then capped with a ~300 nm thick amorphous As cap to protect the *n*-GaAs surface from oxidation before being transferred to another MBE chamber in York for the epitaxial Fe thin film growth. In the second chamber, the GaAs stack was annealed up to 600 °C to thermally desorb the As cap and prepare the pristine GaAs(001) surface for Fe deposition. Figure 1(a) shows typical reflection high-energy electron diffraction (RHEED) patterns of GaAs(001) surface after the *in-situ* annealing, where the sharp streaks indicate highly-ordered crystalline GaAs(001) surfaces prior to the Fe deposition. 5 nm of Fe thin films and Au capping layers were then deposited by MBE at room temperature, where the resultant RHEED patterns in Fig. 1(b) indicates the epitaxial growth relation of GaAs(001)[100]//Fe(001)[100]. In Fig. 1(c), X-ray reflection measurement performed on the sample showed the roughness of the crucial Fe/GaAs interface to be less than 0.5 nm.

The device for the non-local measurements were then fabricated using three-step electron-beam lithography. Firstly, the Fe thin films were etched using Ar-ion milling into rectangular contacts with (1, 4, 20) × 20 μm^2 dimensions, as seen in Fig. 1(d). This process also removes the top 30 nm of the highly-doped GaAs layer (except below the Fe contacts), to confine the electrical current in the lightly-doped GaAs channel layer. This was followed by chemical etching of the GaAs channel layer using an ammonia-based etchant (as the typical sulphuric acid – hydrogen peroxide etchant was found to also etch the Fe contacts) to create the 10 × 100 μm^2 GaAs mesa. Without removing resists, SiO_x passivation layer was deposited by plasma-enhanced chemical vapour deposition to isolate the GaAs from the Cr/Au contacts, deposited by thermal evaporation, to contact the Fe contacts electrically.

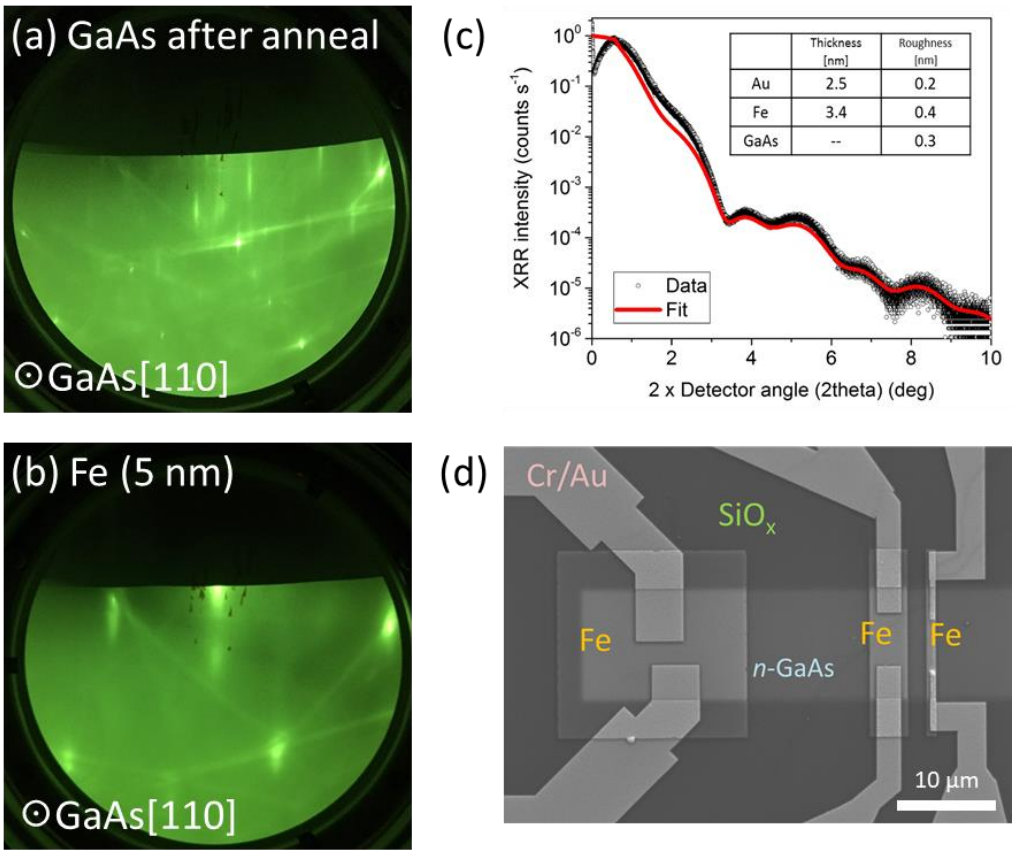

Fig. 1 RHEED (15 keV) images of (a) GaAs(001) after 800ºC anneal and (b) 5 nm deposition of Fe. (c) X-ray reflection measurement of a GaAs/Fe/Au film stack. (d) Scanning electron microscope image of a fabricated four-terminal device.

Results and Discussion

For a successful test of optical gating, efficient electrical spin injection must be achieved first. In order to test the quality of the Fe/*n*-GaAs Schottky barrier at the interface, three-terminal current-voltage characteristic was measured at 4 K, as seen in Fig. 2(a). At the negative bias between the contacts 2 and 4 (*i.e.*, electrons moving from Fe to GaAs), the dc injection current of ~ -1 mA was achieved at around -1 V, as observed similarly in Lou *et al.* [2]. The observed asymmetric *I-V* curve across the Fe/GaAs interface is due to the asymmetric nature of the Schottky barrier, where biasing in opposite directions results in different "effective" widths of the Schottky barrier, as also previously observed [2,15].

The quality of the Fe/GaAs spin injection interface is confirmed by non-destructive scanning electron microscopy (SEM) of the buried interface. Fig. 2(b) shows a non-destructive SEM image of the contacts 1 – 3 with an injection current $I_{2\text{-}1}$ of -125 µA, which was obtained by normalising the contrast difference between the images taken at 2.5 kV and

3 kV deceleration voltage of the sample stage (further details can be found in [16]). Deviations in the SEM image contrast of the injector contacts (highlighted by yellow rectangles in Fig. 2(b)) are normalised by the contrast in the drain contacts (highlighted by green rectangles) and are plotted against the injection current $I_{2\text{-}1}$ and the interface voltage $V_{2\text{-}4}$ in Fig. 2(c). As expected, the deviation is the highest for the lowest injection current, where the transport is expected to be non-uniform, and the contrast deviation decreases (*i.e.*, the transport becomes more uniform) as the injection current/interface bias voltage increases enough to overcome the Schottky barrier height. The large drop of the contrast deviation between the -200 μA and -400 μA injection current suggests that the effective height of the Schottky barrier in this device is ~ 0.45 V, roughly in agreement with previously observed values [17,18]. These results confirm the validity of the non-destructive imaging to assess the corresponding transport properties.

The electrical spin injection was characterised using three- and four-terminal Hanle effect measurements at 4 K, as seen in Fig. 2(d). Here the injection current of -100 μA was applied between the contacts 2 and 1, while the voltages were measured between the two sets of contacts (2-4) and (3-4), respectively. The application of the out-of-plane magnetic field causes the precession and the dephasing of the injected spins (polarised in the plane of the contact/surface). This is characterised by the decrease in the measured voltages with the increasing field strength. By fitting the Lorentzian function to the observed peaks, the spin dephasing time τ_S can be obtained using the following equation:

$$\tau_S = \frac{\hbar}{g\mu_B B_{z,\mathrm{HWHM}}}, \qquad (1)$$

where *g*-factor g of *n*-GaAs is assumed to be -0.44 [19] and $B_{z,\mathrm{HWHM}}$ is the measured half-width at half-maximum from the Hanle peak. A strong in-plane magnetic anisotropy of the Fe strip, required for applying the standard Hanle transport model, was verified using SQUID magnetometry in the Supplemental Material Section II [14]. From the measured half-width at half-maximum of around 440 mT, the spin dephasing is estimated to be 60 ps in our case. This compares with the previously measured spin lifetime of 24 ns at 10 K [2,20], where the short spin dephasing time seen in our Hanle measurement is attributed to the fast dephasing of the carrier spins in the highly-doped ($n = 5 \times 10^{18}$ cm^{-3}) GaAs layer, as seen in Tran *et al.* [21].

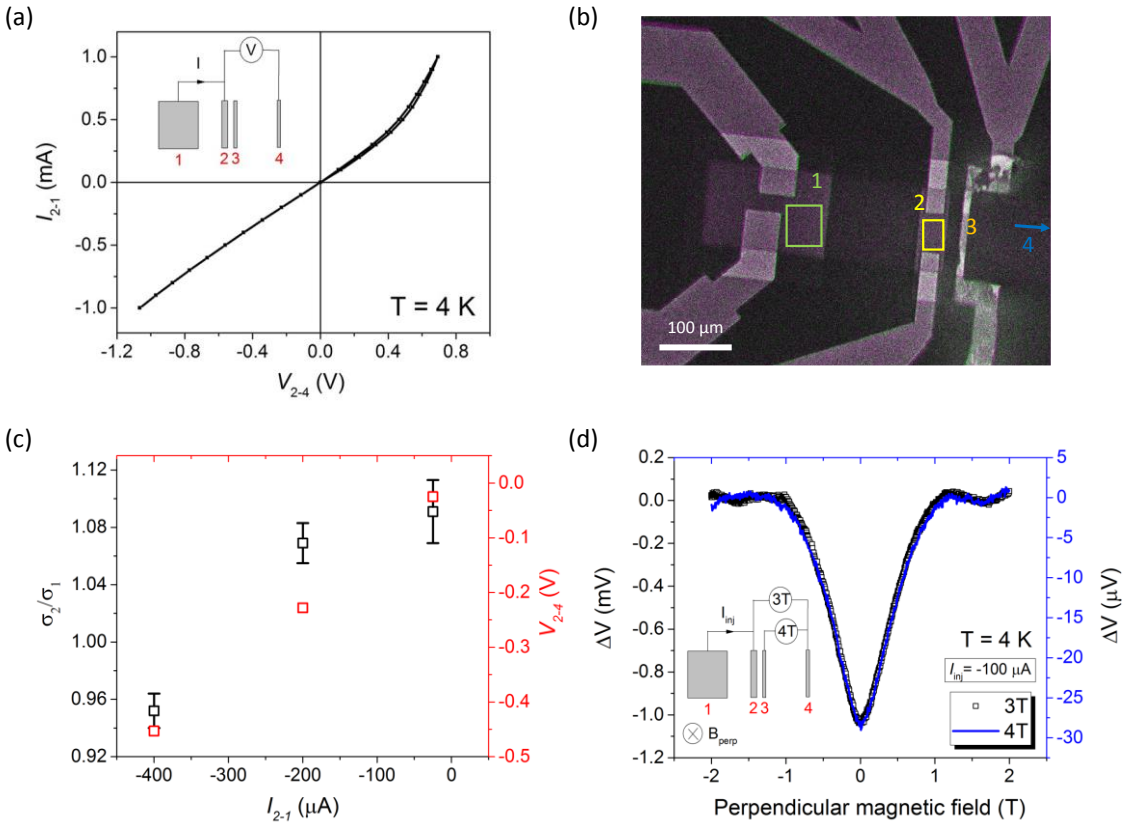

Fig. 2 (a) Three-terminal current-voltage relation of the Fe/GaAs interface of the injection contact (2) as measured at 4 K. (b) *in-situ* SEM interface image of the spin-valve device with an injection current $I_{2\text{-}1}$ of -125 µA where two images with 3.0 kV and 2.5 kV electron-beam deceleration voltages are subtracted to highlight the interface. The yellow and the green rectangles indicate the regions used for contrast deviation analysis of the injector and drain contact, respectively. (c) The injection current $I_{2\text{-}1}$ dependence of the ratio of contrast deviations between the injector (2) and the drain (1) contact, σ_2/σ_1, and the interface voltage $V_{2\text{-}4}$. (d) Three- and Four-terminal Hanle voltages (with offset voltages of -0.137 V and -2.32 mV, respectively) measured with -100 µA injection current at 4 K.

In order to investigate further the spin dephasing time in the *n*-GaAs channel, time-resolved Kerr pump-probe measurements were performed at 30 K. A wavelength-tunable mode-locked pulsed laser with a photo-elastic modulator was used to illuminate a circularly polarised beam to the *n*-GaAs channel, while the time-resolved linearly polarised light was used to measure the Kerr response of the channel. Fig. 3(a) shows the wavelength-dependence of the time-resolved Kerr rotation (TRKR) signal with the applied in-plane magnetic field of 0.65 T at 30 K. The maximum response was observed at around the

wavelength of 822 nm, which corresponds well with the 1.5 eV band-gap of GaAs expected at 30 K [22]. The precession and the dephasing of the optically-injected spins from the Kerr signal at time Δt after the initial excitation can be modelled using the following equation [23]:

$$S_z = S_0 \exp(-\Delta t/\tau_s)\cos(\Omega \Delta t), \quad (2)$$

where S_0 is the initial spin momet (at Δt = 0), and Ω is the precession frequency of the injected spins. The numerial fitting of the Kerr response at the 822 nm excitation wavelength gives the spin dephasing time τ_s of ~ 2.7 ns at 30 K, which is in agreement with the literature values [2,23]. The large discrepancy between the two spin dephasing times obtained from the electrical Hanle and the optical TRKR measurements is thought to be due to the dephasing of the electrically injected spins in the "thickness direction". In order to circumvent this issue, a thinner (800 nm instead of 2 μm) layer of the GaAs channel could be used, as employed by Shiogai *et al.* [24]. In fact, for Si, it is shown that a very thin (70 nm) channel thickness led to a higher spin accumulation possibly due to the confinement of injected spins [25]. To eliminate further spurious sources of the field-dependent signals, non-magnetic metals could be used as the source and the drain contacts for the non-local injection and detection [26].

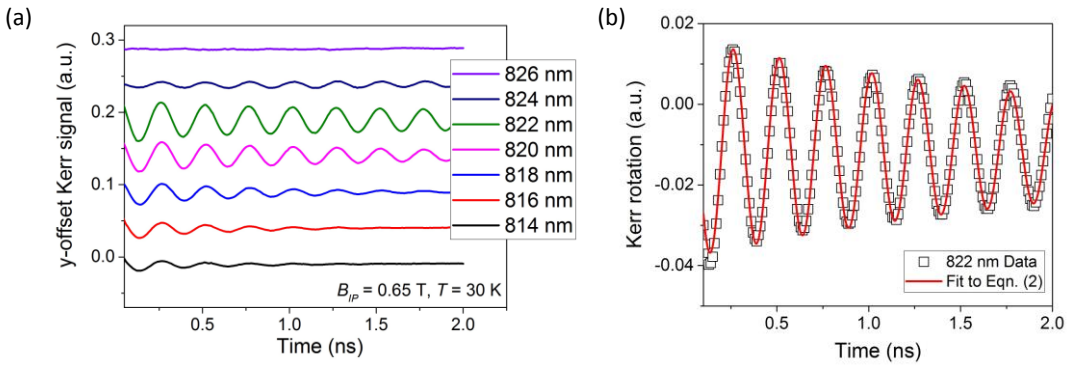

Fig. 3 (a) Wavelength dependence of time-resolved Kerr rotation signals in *n*-GaAs at 30 K. (b) Numerical fit of 822 nm Kerr response to Equation (2).

As the key step to test the feasibility of the optical gating of the non-local spin transport, the circularly-polarised light at the 822 nm wavelength was illuminated to the region of pure spin current between the injector and the detector ferromagnets as shown in Fig. 4(a). This is similar to the conventional electric field gate applications of the Datta-Das-type spin field-effect transistor [1,27], where instead of the electric field the circularly-polarised light is used to modulate the non-local voltage. Figure 4(b) shows the optical micrograph of the spin injection device, where the red circle indicates the region of the non-local spin transport where the circularly-polarised light was illuminated. Figure 4(c) shows the dependence of the

non-local voltage measured between the contacts 3 and 4, with different laser power and the polarisation of the modulation light, measured at 30 K. Systematic differences in the non-local transport signal between the cases of the clockwise (red) and the counter-clockwise (blue) circular polarisation start to appear with increasing laser power. This is better seen in Fig. 4(d), where the ratio of the difference and the sum of the signals with the two opposite polarisation, $(V_{\sigma+} - V_{\sigma-})/|(V_{\sigma+} + V_{\sigma-})|$, is plotted against the laser power. At 7 mW laser power, the ratio, which can be regarded as the optical modulation efficiency, reaches (0.4 ± 0.3)%. This indicates that the spins of the photoexcited carriers are sufficient to modify the accumulation underneath the detector contact directly. This efficiency is comparable to ~1% modulation efficiency obtained at 2 K by Koo *et al.* [27] via electric-field gating in NiFe/InAs structure, and could increase further with a higher laser power at lower temperatures. Due to the vectorial nature of our gating scheme, where the measured signal depends on the relative angle between the detector magnetisation and the accumulated spin polarisation, an oscillatory behaviour with the light intensity is expected. However, the small differential signals compared with the measurement errors rule out a conclusive observation of the effect at this stage. As can be seen from the large modulation efficiency of the Ampère-field-generating current-gating of a nanometric nano-ring [28], the miniaturisation of our devices is expected to increase our modulation efficiency. The optical gating technique in our structure could have a significant advantage over conventional electric-field gating due to a lower power consumption up to 25% [29].

In the current configuration, the laser spot size was measured to be ~ 20 μm in diameter, which is almost the same as the GaAs mesa width, and around ten times larger the GaAs area between the Fe electrodes. By tuning the spot size, the efficiency can be enhanced further. In addition, both the spot size and the GaAs mesa can be reduced with maintaining the efficiency, which paves a way towards a nanometric spin FET. This cannot be achieved using the conventional electric and magnetic gating.

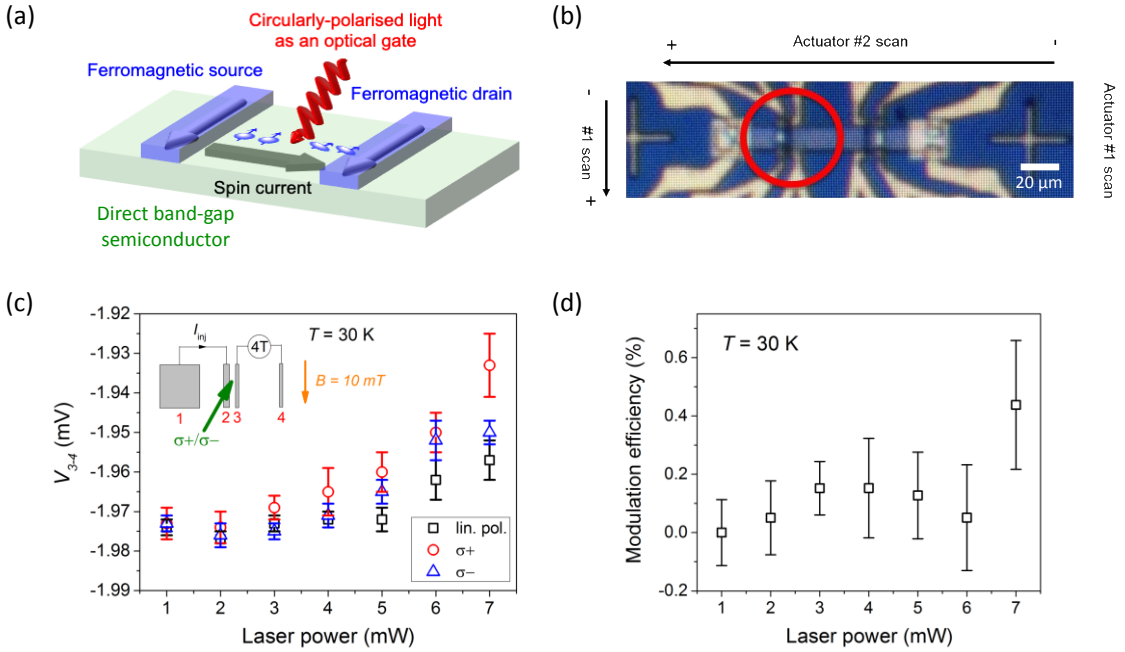

Fig. 4 (a) Schematic of the optical gating in non-local spin injection devices. (b) The optical micrograph of our device in the optical cryostat used for the time-resolved Kerr measurements. The red circle indicates the region of the circularly-polarised light excitation. (c) Non-local voltage (measured between the contacts 3 and 4 with I_{inj} = - 100 μA at 30 K) with the clockwise (red) and the counter-clockwise (blue) circular polarisations and the linear polarisation (black) (d) Optical modulation efficiency, as defined as the percentage ratio of the difference and the sum of the non-local voltages with the clockwise and the counter-clockwise circular polarisation, $(V_{3-4,\sigma+} - V_{3-4,\sigma-})/(V_{3-4,\sigma+} + V_{3-4,\sigma-})$, against the laser power.

Conclusion

We have successfully demonstrated efficient optical gating on electrical spins injected in Fe/*n*-GaAs with narrow Schottky barriers. Contrast variation analysis of the *in-situ* SEM interfacing images allows non-invasive probing of the injector interface uniformity. Three- and four-terminal Hanle measurements reveal the fast spin dephasing time in the highly-doped *n*-GaAs layer at high magnetic fields. Time-resolved pump-probe Kerr rotation measurement was performed to demonstrate the optically-injected spins in the lightly-doped *n*-GaAs channel layer where the highest excitation was observed at 822 nm at 30 K. Helicity-dependent variation of non-local signal with optical gating is observed with the modulation efficiency of (0.4 ± 0.3)% at 30 K, which may increase further with higher laser power at lower temperature. Due to the controllability of optical spot size, this method can offer efficient gating in nanometric scale, which has not been achieved with the conventional electric and

magnetic gating.

Acknowledgements

This work was partially supported by EPSRC Programme (EP/M02458X/1) and JST PRESTO and CREST (No. JPMJCR17J5). J.-Y. K. acknowledges the JSPS Core-to-Core programme for the research visits to Tohoku University, the Deutsche Forschungsgemeinshaft (DFG, German Research Foundation) – TRR 173 – 268565370 (project B02), the National Research Foundation Competitive Research Programs (NRF-CRP24-2020-0002) and Agency for Science, Technology and Research (A*STAR) Science and Engineering Research Council (SC25/21-7078D1).

References

[1] S. Datta and B. Das, *Electronic Analog of the Electro□optic Modulator*, Appl. Phys. Lett. **56**, 665 (1990).

[2] X. Lou, C. Adelmann, S. A. Crooker, E. S. Garlid, J. Zhang, K. S. M. Reddy, S. D. Flexner, C. J. Palmstrøm, and P. A. Crowell, *Electrical Detection of Spin Transport in Lateral Ferromagnet–Semiconductor Devices*, Nat. Phys. **3**, 197 (2007).

[3] G. Salis, A. Fuhrer, R. R. Schlittler, L. Gross, and S. F. Alvarado, *Temperature Dependence of the Nonlocal Voltage in an Fe/GaAs Electrical Spin-Injection Device*, Phys. Rev. B **81**, 205323 (2010).

[4] O. Wunnicke, Ph. Mavropoulos, R. Zeller, P. H. Dederichs, and D. Grundler, *Ballistic Spin Injection from Fe(001) into ZnSe and GaAs*, Phys. Rev. B **65**, 241306 (2002).

[5] S. A. Crooker, *Imaging Spin Transport in Lateral Ferromagnet/Semiconductor Structures*, Science **309**, 2191 (2005).

[6] S. Honda, H. Itoh, J. Inoue, H. Kurebayashi, T. Trypiniotis, C. H. W. Barnes, A. Hirohata, and J. A. C. Bland, *Spin Polarization Control through Resonant States in an Fe/GaAs Schottky Barrier*, Phys. Rev. B **78**, 245316 (2008).

[7] L. R. Fleet, K. Yoshida, H. Kobayashi, Y. Kaneko, S. Matsuzaka, Y. Ohno, H. Ohno, S. Honda, J. Inoue, and A. Hirohata, *Correlating the Interface Structure to Spin Injection in Abrupt Fe/GaAs(001) Films*, Phys. Rev. B **87**, 024401 (2013).

[8] P. R. Hammar, B. R. Bennett, M. J. Yang, and M. Johnson, *Observation of Spin Injection at a Ferromagnet-Semiconductor Interface*, Phys. Rev. Lett. **83**, 203 (1999).

[9] B. T. Jonker, G. Kioseoglou, A. T. Hanbicki, C. H. Li, and P. E. Thompson, *Electrical Spin-Injection into Silicon from a Ferromagnetic Metal/Tunnel Barrier Contact*, Nat. Phys. **3**, 542 (2007).

[10] W. Y. Choi, H. Kim, J. Chang, S. H. Han, H. C. Koo, and M. Johnson, *Electrical Detection*

of Coherent Spin Precession Using the Ballistic Intrinsic Spin Hall Effect, Nat. Nanotechnol. **10**, 666 (2015).

[11] A. Hirohata, K. Yamada, Y. Nakatani, I.-L. Prejbeanu, B. Diény, P. Pirro, and B. Hillebrands, *Review on Spintronics: Principles and Device Applications*, J. Magn. Magn. Mater. **509**, 166711 (2020).

[12] S. Maekawa, S. O. Valenzuela, and E. Saitoh, editors , *Spin Current*, Second edition (Oxford University Press, Oxford, United Kingdom, 2017).

[13] G. Snider, *1-Dimensional Poisson/Schrödinger Band Diagram Calculator*, (n.d.).

[14] *See Supplemental Material at [URL Will Be Inserted by Publisher] for Additional Details on 1-d Band Diagrams of Fe/n-GaAs Interface and a Comparison of Fe Contact out-of-Plane Anisotropic Magnetoresistance with Hanle Data.*, (n.d.).

[15] S. Sinha, S. Kumar Chatterjee, J. Ghosh, and A. Kumar Meikap, *Semiconducting Selenium Nanoparticles: Structural, Electrical Characterization, and Formation of a Back-to-Back Schottky Diode Device*, J. Appl. Phys. **113**, 123704 (2013).

[16] E. Jackson et al., *Non-Destructive Imaging for Quality Assurance of Magnetoresistive Random-Access Memory Junctions*, J. Phys. Appl. Phys. **53**, 014004 (2019).

[17] H. Kurebayashi, S. J. Steinmuller, J. B. Laloë, T. Trypiniotis, S. Easton, A. Ionescu, J. R. Yates, and J. A. C. Bland, *Initial/Final State Selection of the Spin Polarization in Electron Tunneling across an Epitaxial Fe⁄GaAs(001) Interface*, Appl. Phys. Lett. **91**, 102114 (2007).

[18] L. R. Fleet, H. Kobayashi, Y. Ohno, J.-Y. Kim, C. H. W. Barnes, and A. Hirohata, *Interfacial Structure and Transport Properties of Fe/GaAs(001)*, J. Appl. Phys. **109**, 07C504 (2011).

[19] M. Oestreich and W. W. Rühle, *Temperature Dependence of the Electron Land¥'e $¥mathit{g}$ Factor in GaAs*, Phys. Rev. Lett. **74**, 2315 (1995).

[20] S. H. Nam, T.-E. Park, Y. H. Park, H.-I. Ihm, H. C. Koo, H. Kim, S. H. Han, and J. Chang, *Spin Accumulation at In-Situ Grown Fe/GaAs(100) Schottky Barriers Measured Using the Three- and Four-Terminal Methods*, Appl. Phys. Lett. **109**, 122409 (2016).

[21] M. Tran, H. Jaffrès, C. Deranlot, J.-M. George, A. Fert, A. Miard, and A. Lemaître, *Enhancement of the Spin Accumulation at the Interface between a Spin-Polarized Tunnel Junction and a Semiconductor*, Phys. Rev. Lett. **102**, 036601 (2009).

[22] M. B. Panish and H. C. Casey, *Temperature Dependence of the Energy Gap in GaAs and GaP*, J. Appl. Phys. **40**, 163 (1969).

[23] J. M. Kikkawa and D. D. Awschalom, *Resonant Spin Amplification in n -Type GaAs*, Phys. Rev. Lett. **80**, 4313 (1998).

[24] J. Shiogai, M. Ciorga, M. Utz, D. Schuh, M. Kohda, D. Bougeard, T. Nojima, J. Nitta, and D. Weiss, *Giant Enhancement of Spin Detection Sensitivity in (Ga,Mn)As/GaAs Esaki Diodes*, Phys. Rev. B **89**, 081307 (2014).

[25] A. Spiesser, H. Saito, Y. Fujita, S. Yamada, K. Hamaya, S. Yuasa, and R. Jansen, *Giant Spin Accumulation in Silicon Nonlocal Spin-Transport Devices*, Phys. Rev. Appl. **8**, 064023 (2017).

[26] L.-K. Liefeith, R. Tholapi, M. Hänze, R. Hartmann, T. Slobodskyy, and W. Hansen, *Influence of Thermal Annealing on the Spin Injection and Spin Detection through Fe/GaAs Interfaces*, Appl. Phys. Lett. **108**, 212404 (2016).

[27] H. C. Koo, J. H. Kwon, J. Eom, J. Chang, S. H. Han, and M. Johnson, *Control of Spin Precession in a Spin-Injected Field Effect Transistor*, Science **325**, 1515 (2009).

[28] B. A. Murphy, A. J. Vick, M. Samiepour, and A. Hirohata, *Highly Efficient Spin-Current Operation in a Cu Nano-Ring*, Sci. Rep. **6**, 37398 (2016).

[29] A. Hirohata, *Spin Polarization Transistor Element*, US9190500B2 (17 November 2015).